Hydrogeol J
DOI 10.1007/s10040-016-1439-2

PAPER

Using multiple environmental methods to estimate groundwater discharge into an arid lake (Dakebo Lake, Inner Mongolia, China)

Xiaosi Su [1,2] · Geng Cui [1,2] · Shanghai Du [1,2] · Wenzhen Yuan [1,2] · Huang Wang [1,2]

Received: 21 December 2015 / Accepted: 12 June 2016

Abstract It is important to have both a qualitative and quantitative understanding of the hydraulic exchange between groundwater and surface water to support the development of effective management plans for sustainable use of water resources. Groundwater is a major source of surface-water recharge and plays an important role in maintaining the integrity of ecosystems, especially within wetlands in semi-arid regions. The Ordos Desert Plateau of Inner Mongolia (China) is a vulnerable ecosystem that suffers from an extreme lack of water. The hydraulic exchange between groundwater and lake water in Dakebo Lake (the largest of hundreds of lakes on the Ordos Desert Plateau) was evaluated using multiple environmental methods. Continuous monitoring of the groundwater and lake-water levels indicated that the lake was recharged vertically by groundwater. Application of hydrodynamic and temperature tracing methods to the western side of the lake indicated that the rate of groundwater discharge to the lake was about 2×10^{-6} to 3×10^{-6} m/s in spring, summer, and autumn, but that there was no recharge in winter because the hypolentic zone (HZ) was frozen. Mixing ratios of groundwater and lake water in the HZ, estimated from the ^{18}O and ^{2}H ratios, showed that there were spatial variations in the hydrodynamic exchange between groundwater and lake water within the HZ.

✉ Shanghai Du
yoko_sh@yeah.net

[1] Key Laboratory of Groundwater Resources and Environment, Ministry of Education, Jilin University, Changchun 130021, China

[2] Institute of Water Resources and Environment, Jilin University, Changchun 130021, China

Keywords Hypolentic zone · Temperature tracing · Stable isotopes · China · Groundwater/surface-water relations

Introduction

Playa lakes often occur in arid and semi-arid climates and have significant economic, ecological and cultural value. They are particularly fragile and sensitive to variations in hydrological conditions caused by climate change and human activities (Rodríguez-Rodríguez et al. 2006; Du et al. 2013; Su et al. 2015). Studies have shown that various interactions occur between groundwater and surface water under natural conditions and in response to human activities via a constant transmission of water, solutes, nutrients and energy (Sophocleous 2002; Su et al. 2014a, b).

Wetland ecosystems will form where there is low-lying terrain and a sustained water source. Lakes, a form of wetland, are particularly dependent on groundwater discharge in arid and semi-arid areas because of the high evaporation rates and limited rainfall (Rodríguez-Rodríguez et al. 2006; Wang et al. 2003). Groundwater flows have a major role in maintaining the ecosystems of high elevation lakes by providing aquatic species with oxygen, nutrients, and essential chemical elements during late winter and early spring (Shaw et al. 2013). Therefore, it is important to have an understanding of the interactions between groundwater and lakes to be able to protect the ecosystems in arid and semi-arid regions (Li et al. 2016).

As a mixing zone of surface water and groundwater dominated by biogeochemical activities, the hypolentic zone (HZ) can effectively: degrade toxic or harmful substances; purify surface water or groundwater (Gandy et al. 2007); change the acidity, redox potential, and dissolved oxygen content of water flowing through the HZ; and protect ecosystems from

Published online: 29 June 2016

interference by external factors (Zalewski 2000). For example, the temperature gradient in the HZ can provide a heat buffer for surface water and groundwater exchange and habitats and shelters for specific creatures (Sedell et al. 1990; Grimm and Fisher 1984). Therefore, the HZ, as the interface between surface water and groundwater, is important to ecosystems and its protection is an issue of increasing importance in many international scientific research programs.

Energy, materials, and salinity are conveyed via hydrodynamic exchanges from groundwater to the surface water within the HZ; hydrodynamic exchanges are therefore important drivers of the migration and transformation of substances and biochemical processes (Shaw et al. 2013; Lee et al. 2014; Elsawwaf et al. 2014; Rautio and Korkka-Niemi 2015). However, to date, studies of surface-water/groundwater exchanges have mainly focused on the HZ in rivers (Keery et al. 2007; Storey et al. 2003), and there has been a lack of studies on the HZ of lakes. Because the conditions in the HZ of lakes and rivers are significantly different, exchanges between groundwater and lake water need to be explored and defined, especially in desert plateau lakes with extreme climates.

Currently, three main methods are used to estimate hydrodynamic exchanges between groundwater and surface water: the hydrodynamic method (Kalbus et al. 2006), environmental isotope tracing method (Carey and Quinton 2005; Yin et al. 2011; Oyarzún et al. 2014), and thermal tracing method (Hatch et al. 2006; Essaid et al. 2008; Rau et al. 2014). Isotopes of ^{18}O and ^{2}H are widely used because their isotopic compositions differ markedly between water sources and they are not influenced by other factors during the mixing process (Marimuthu et al. 2005). The thermal tracing method has gained popularity as temperature-measuring devices have been developed and thermal simulation methods have been advanced (Constantz et al. 2008). As a natural tracer, temperature is an environmentally friendly cost-effective parameter that is easily measured and provides reliable results. It is now one of the main methods used to calculate groundwater/surface-water exchanges. Multidisciplinary theory and methods can be combined to effectively investigate groundwater/surface-water interactions and to assess responses to change at the groundwater/surface-water interface; to date, a range of studies have been carried out to further develop this combined approach (Fan et al. 2012).

The Ordos Desert Plateau, in the Inner Mongolia Autonomous Region of China, is a very fragile ecosystem characterized by an extreme lack of surface water. Lake wetlands are the main datum plane of regional groundwater, and are also an important part of the Ordos Relict Gull National Nature Reserve. The water quantity and quality of the lake wetlands in this region play an important role in maintaining natural resources and ecosystems of the lakes. Therefore, determining the groundwater discharge to lakes is particularly important for understanding the supply resources of lake water.

Many detailed hydrogeological investigations have been carried out in Dakebo Lake, one of the largest lakes in the study area, and its surroundings since 2010. For example, Su et al. (2011) studied the groundwater/lake-water exchange and the transformation of hydrochemical components of pore water in the Dakebo Lake region of the Ordos Desert Plateau using hydrochemistry and isotope tracing. Wang (2011) identified the characteristics and influencing factors of groundwater evolution, hydrochemistry, and isotopes of the Dakebo Lake region in Ordos Basin. In addition, previous studies divided the study area into three groundwater flow systems—namely local, intermediate, and regional (Cao 2009). Dakebo Lake is in a typical local groundwater flow system, but no detailed observed data have confirmed these findings and there have been few in-depth studies of the amount of flow from each system. Accordingly, no clear strategy has been developed to protect these lake wetlands.

In this study, the sources of pore water, and the pattern and intensity of the hydraulic exchange within the HZ of Dakebo Lake were identified from the stable isotopes of different sources of pore water. The various measured values of the deuterium and oxygen isotopic compositions of pore water within the HZ were used to identify the hydraulic exchange pattern, calculate the mixing ratios of different water bodies at different depths below the lakebed, and separate the hydrodynamic exchange zones. In addition, the amount of exchange between groundwater and lake water was quantified by the hydrodynamic method. Specifically, the exchange was calculated using the temperature tracing method and Darcy's Law with dynamic data that described the temperature and water levels of groundwater and lake water.

Hydrogeological setting

The study area is a small basin in Etuokeqi Territory of the Inner Mongolia Autonomous Region, in the center of the northern part of Ordos Basin that has an elevation between 1,330 and 1,505 m above sea level (Fig. 1). Dakebo Lake is in the center of the basin and because it has the lowest elevation, it accepts groundwater discharge from the surrounding area. Analysis of meteorological data from the Etuokeqi Meteorological Station showed that the average annual precipitation in the study area is only 265 mm, most of which occurs from June to September of each year. The average annual evaporation reaches 2,506 mm, and evaporation is most intense from April to August. The groundwater is mainly stored in the Quaternary aquifer, which contains lacustrine and aeolian deposits of sand, and the Cretaceous aquifer, which contains sandstone, mudstone, and conglomerate. The main landforms include wind-accumulated landforms, lake beaches, and a bedrock platform. The lithological properties and aquifer media indicate that the groundwater bodies can be roughly

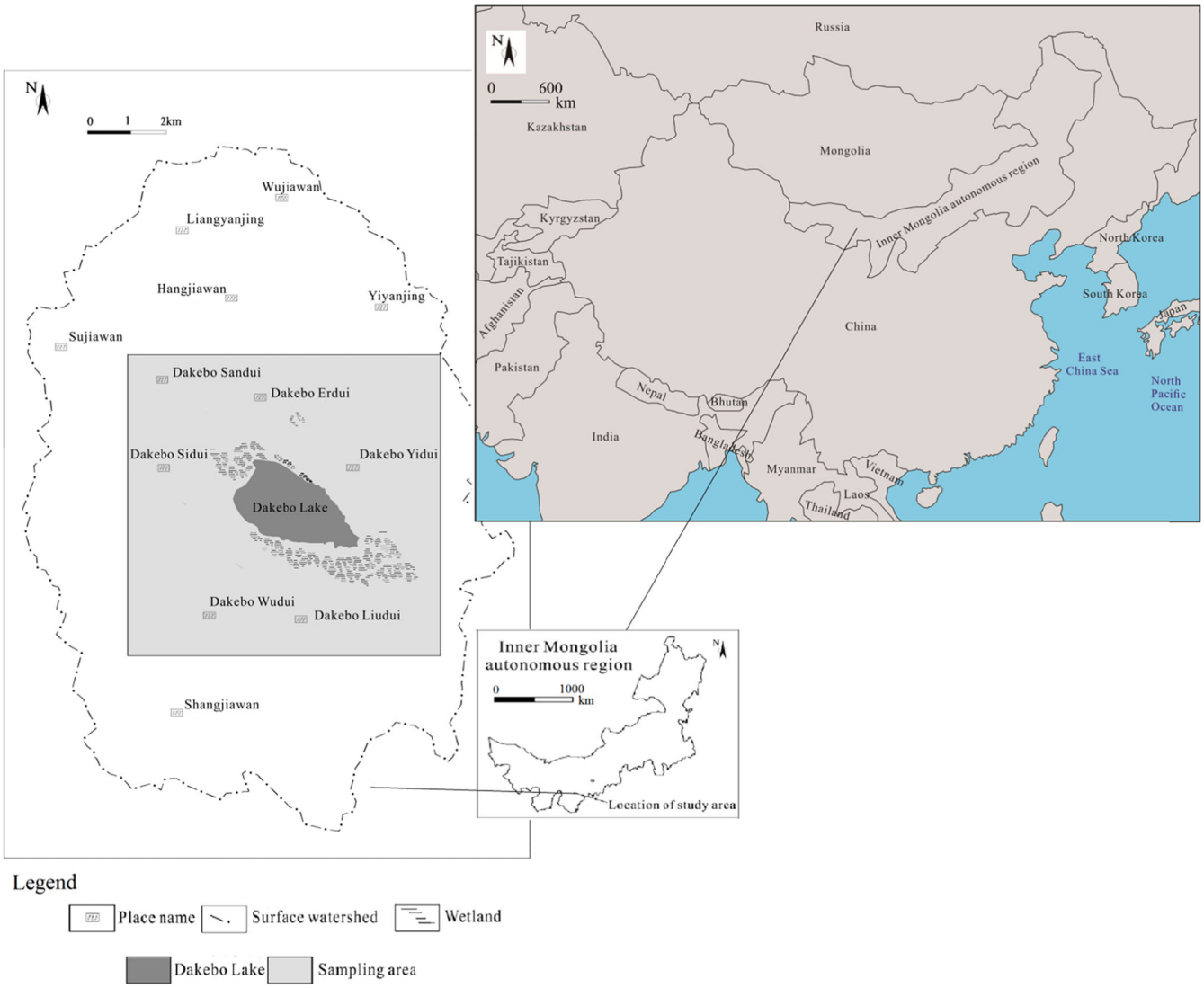

Fig. 1 Location map of the study area

divided into shallow groundwater, middle groundwater, and deep groundwater. The horizontal and vertical zonation characteristics of the lithology of Dakebo Lake and the proximal lakeshore sediment were determined from shallow boreholes (Fig. 2). There are horizontal areas comprised mainly of sandy loam on both sides of the lake, while there is a layer of silty loam below the lakebed that gradually thickens from east to west. The area below the lakebed is mainly composed of silty loam; however, there is a thin layer of clay loam spreading at the center of the lake. This silty loam layer is underlain by sandy loam.

Because of ongoing deposition of wind-blown sand from the nearby dunes, a thin sand layer has developed at the western side of the lake. Groundwater in the study area is generally recharged by infiltration of precipitation, seepage of agricultural irrigation and lateral flow. There is a layer of loose Quaternary sediments in this area that is conducive to recharge by precipitation. Agricultural irrigation seepage mainly occurs about 1 km away from Dakebo Lake, and shows an annular distribution; however, the agricultural irrigation seepage has become negligible because of population migration out of the region. Groundwater flow is mainly controlled by the terrain. Groundwater flows from the surrounding watershed to Dakebo Lake because surrounding topography slopes toward the lake (Fig. 3). Groundwater is recharged by precipitation in peripheral areas of the lake where there is enhanced permeability, and then the lake water is recharged by groundwater, driven by the hydraulic gradient. Groundwater flow shows vertical discharge at the center of the lake and vertical and lateral discharge to the lakeshore.

Methods

Monitoring wells

To carry out comprehensive monitoring of the hydrodynamics within the hypolentic zone of Dakebo Lake, three monitoring

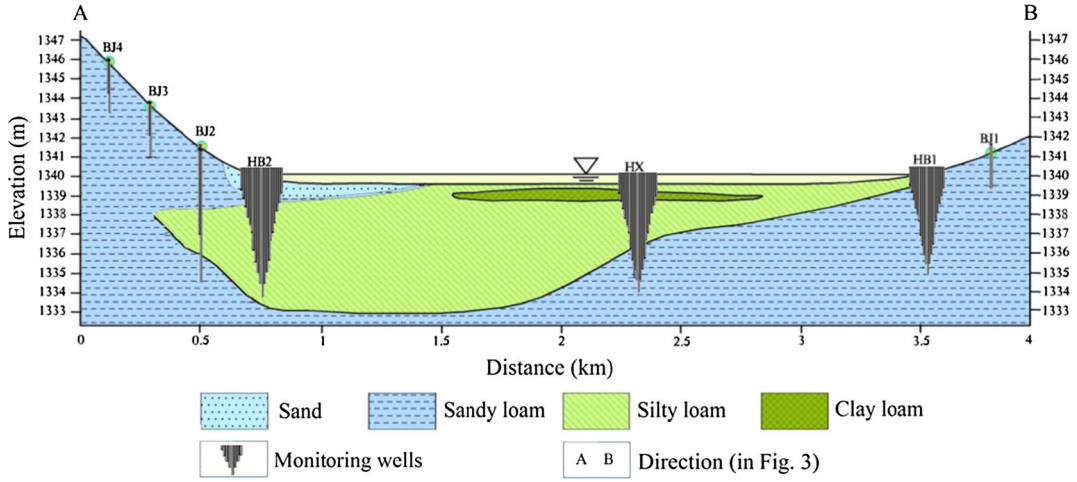

Fig. 2 Hydrogeologic profile of the shallow aquifer below the lakebed and the sectional view of monitoring wells

sites were established: at the center (No. HX), and on the eastern (No. HB1) and western (No. HB2) sides of the lake. Monitoring wells were also arranged on both the eastern and western sides of the section, one on the eastern shore (No. BJ1) and six on the western shore (Nos. BJ*-1, BJ*-2, BJ*-3, BJ2, BJ3, BJ4; Fig. 3). Wells of different depths were established within the HZ of the three main monitoring sites (HB1, HX, HB2) so that the groundwater levels and the stable isotopic compositions of ^{18}O and ^{2}H could be measured at different depths, and to collect other relevant information at

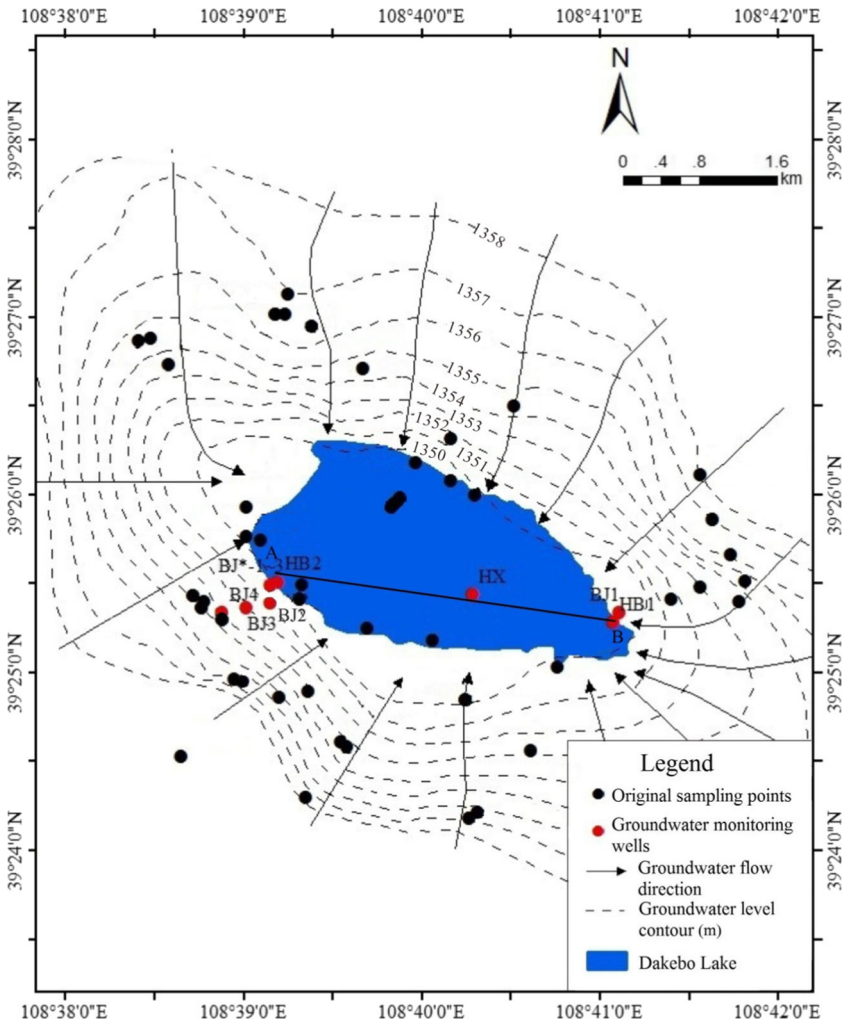

Fig. 3 Groundwater flow around, and distribution of monitoring sites within Dakebo Lake

different depths (Fig. 2). To take account of the decreasing vertical gradient in the mixing ratios of the different water bodies, and the hydrochemical composition and other environmental indicators within the HZ (Guo 2012), the depth intervals of the wells vary in different ranges, thereby contributing to a well cluster system at the three main monitoring sites (HB1, HX, HB2). The main parameters of the monitoring wells are shown in Table 1. The casing diameter of all the wells is 10 cm.

Water level and temperature monitoring

To analyze and evaluate the amount of groundwater/lake-water exchange, and to monitor the surrounding groundwater and pore water at different depths within the HZ, seven self-recording water level loggers (dipperLog, Heron Instruments Inc., Ontario, Canada) were placed at the center (HX) and on the western side (HB2) of the lake in September 2012. More specifically, two of these loggers were positioned in the center of the lake at HX-14 (1 m deep) and HX-4 (5 m deep), one was placed on the western side of the lake at HB2-15 (0.9 m deep), and four were placed on the boundary of the western side of the lake at sites BJ2-2 (3 m deep, 200 m from the lake), BJ*-1 (2 m deep, 10 m from the lake), BJ*-2 (2 m deep, 15 m from the lake), and BJ*-3 (2 m deep, 20 m from the lake).

A temperature monitoring profile was also established at HB2 to obtain continuous water temperature data automatically with water-temperature-data loggers (TidbiT v2, UTBI-001 Onset INC., USA). Temperatures were recorded every 15 min at depths of 0, 0.1, 0.2, 0.3, 0.4, 0.6, 0.8, 1, 1.2, 1.6, 2, 2.5 and 3 m below the surface at a precision of 0.02 °C (Fig. 4).

Isotope sampling

Sixty-six samples of groundwater and lake water were collected in July 2013 for water quality and isotopic (δ^2H, $\delta^{18}O$) analysis with a water pump (Mega-Typhoon, Proactive Environmental Products, Bradenton, FL, USA). The pump is equipped with a professional ECT (electronic control transmission) controller and can achieve stable low-flow sampling

Table 1 Well depths and construction details

Well No.	Hole depth (m)	Depth of screen sections (m)	Seal depths (m)	
			Bottom seal	Top seal
HB2-3	7.5	6.5–5.5	7.5–6.5	5.5–4.5
HB1-4	7	6.0–5.0	7.0–6.0	5.0–4.0
HX-4	6	5.0–4.0	6.0–5.0	4.0–3.0
HB2-4	5.5	4.5–4.0	5.5–4.5	4.0–3.5
HB1-6\HX-6	4.5	3.5–3.0	4.5–3.5	3.0–2.0
HB1-7\HB2-7\HX-7	4	3–2.5	4–3.0	2.5–1.5
HB1-8\HB2-8\HX-8	3.5	2.5–2.0	3.5–2.5	2.0–1.0
HB1-9\HB2-9\HX-9	3	2.0–1.8	3.0–2.0	1.8–0.8
HB1-10\HB2-10\HX-10	2.8	1.8–1.6	2.8–1.8	1.6–0.6
HB1-11\HB2-11\HX-11	2.6	1.6–1.4	2.6–1.6	1.4–0.4
HB1-12\HB2-12\HX-12	2.4	1.4–1.2	2.4–1.4	1.2–0.2
HB1-13\HB2-13\HX-13	2.2	1.2–1.0	2.2–1.2	1.0–0
HB1-14\HB2-14\HX-14	2	1.0–0.9	2.0–1.0	0.9–0
HB1-15\HB2-15\HX-15	1.9	0.9–0.8	1.9–0.9	0.8–0
HB1-16\HB2-16\HX-16	1.8	0.8–0.7	1.8–0.8	0.7–0
HB1-17\HB2-17\HX-17	1.7	0.7–0.6	1.7–0.7	0.6–0
HB1-18\HB2-18\HX-18	1.6	0.6–0.5	1.6–0.6	0.5–0
HB1-19\HB2-19\HX-19	1.5	0.5–0.4	1.5–0.5	0.4–0
HB1-20\HB2-20\HX-20	1.4	0.4–0.3	1.4–0.4	0.3–0
HB1-21\HB2-21\HX-21	1.3	0.3–0.2	1.3–0.3	0.2–0
HB1-22\HB2-22\HX-22	1.2	0.2–0.1	1.2–0.2	0.1–0
HB1-23\HB2-23\HX-23	1.1	0.1–0	1.1–0.1	0–0.1
BJ1\BJ2-2	3	3.0–1.0	–	–
BJ2-1	7	7.0–6.0	–	6.0–5.0
BJ3-1\BJ4-1	3	3.0–2.5	–	2.5–1.5
BJ3-2\BJ4-2	1.5	1.5–0.5	–	–
BJ*-1\BJ*-2\BJ*-3	2	2.0–0	–	–

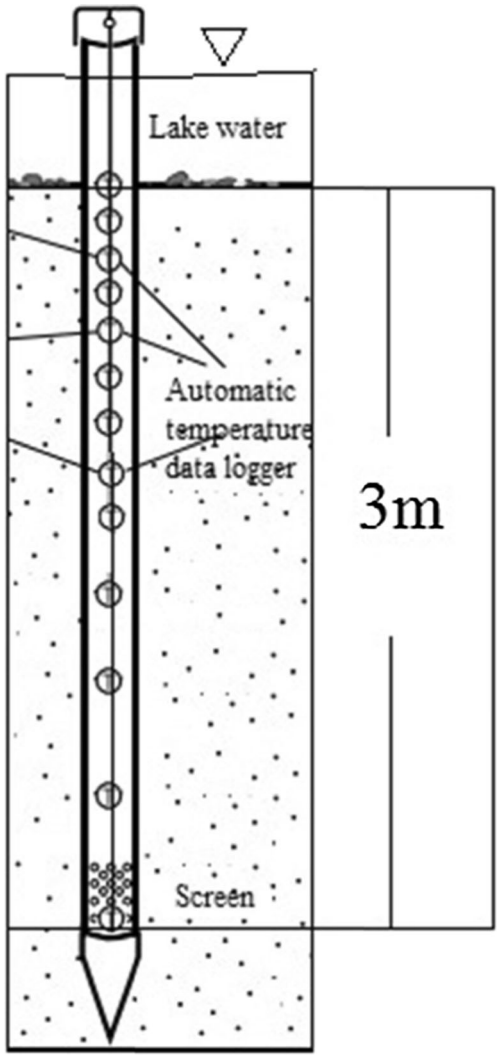

Fig. 4 Profile of temperature monitoring equipment

with a minimum sampling rate of 0.95 L/min, effectively avoiding changes in variable indexes such as oxidation-reduction potential (Eh) and dissolved oxygen (DO) that result from severe disturbances during the sampling process. The sample collection was finished when the indicators (Eh, DO) stabilized after the well was flushed. Samples were immediately poured into polyethylene bottles that had been pre-cleaned with deionized water, after which the bottles were preserved with a sealing membrane. The isotopic compositions of the samples were determined using a liquid water isotope analyzer (Picarro L1102-i) in the Laboratory of Water Isotope and Water Rock Reactions, at the Institute of Geology and Geophysics, Chinese Academy of Sciences.

Calculation of the mixing ratio of the different end-member water bodies

The hydrodynamic intensity and range of the hydrodynamic exchange zone of pore water within the HZ can be determined by calculating the mixing ratio of groundwater and lake water. Depending on the isotope mass balance principle, the composition of isotopes in the water composed of mixtures of two samples with different isotope values can be determined by:

$$\begin{cases} \delta_1 n_1 + \delta_2 n_2 = \delta(n_1 + n_2) \\ n_1 + n_2 = 1 \end{cases} \quad (1)$$

where δ_1 refers to the isotopic values in one end member, δ_2 refers to the isotopic values in another end member, and δ refers to the isotopic values in the mixing end member; n_1 and n_2 are the mixing ratios of the different end-member water bodies in the pore water.

Hydraulic conductivity and hydraulic gradient

The hydraulic conductivities of the HZs in the area were obtained from 36 slug tests in wells of different depths (Table 2), while the hydraulic gradient (I) was calculated from the pore water, surrounding groundwater and lake-water level data. An isotropic HZ medium was assumed during the calculation. A vertical equivalent hydraulic conductivity was applied because there were vertical and horizontal differences in the lithologies of the HZ.

The vertical hydraulic conductivity (m/s) was calculated by:

$$K_v = \frac{\sum_{i=1}^{n} M_i}{\sum_{i=1}^{n} \frac{M_i}{K_i}} \quad (2)$$

where K_i and M_i are the hydraulic conductivity (m/s) and the thickness (m) of the i-th layer. The vertical equivalent hydraulic conductivities of HB2 and HX were 54.34 and 6.33 cm/day, respectively.

Conversion of the freshwater head of variable-density groundwater and deformation of Darcy's Law

The classical form of Darcy's Law, defined in terms of the hydraulic head, and hence, the intuitive field method, does not apply to groundwater of variable density. Density variations can result from differences in temperature or pressure but more often are caused by differences in solute concentration. To calculate the vertical flux from groundwater to lake water, the point water head, which is obtained by measuring the level of the water–air interface in a groundwater observation well, should be corrected into the freshwater head (Post et al. 2007):

$$h_{f,i} = \frac{\rho_i}{\rho_f} h_i - \frac{\rho_i - \rho_f}{\rho_f} z_i \quad (3)$$

Table 2 Results of slug tests

Well No.	Media thickness (m)	Hydraulic conductivity (m/s)
HB1-10	0.2	6.44E-06
HB1-12	0.2	4.35E-07
HB1-13	0.2	2.65E-06
HB1-15	0.1	2.53E-06
HB1-16	0.1	4.57E-06
HB1-17	0.1	1.71E-06
HB1-18	0.1	1.80E-06
HB1-19	0.1	1.91E-06
HB1-20	0.1	1.42E-06
HB1-21	0.1	1.02E-05
HB2-10	0.2	2.10E-06
HB2-11	0.2	3.66E-06
HB2-12	0.2	1.23E-05
HB2-13	0.2	1.42E-05
HB2-14	0.1	9.48E-06
HB2-15	0.1	5.83E-06
HB2-16	0.1	1.41E-05
HB2-17	0.1	4.55E-06
HB2-18	0.1	4.95E-06
HB2-19	0.1	8.36E-06
HB2-21	0.1	5.88E-06
HB2-22	0.1	1.18E-04
HB2-7	0.5	2.57E-07
HB2-9	0.2	3.70E-06
HX-06	0.5	1.05E-07
HX-07	0.5	6.07E-06
HX-08	0.5	5.43E-07
HX-09	0.2	1.10E-05
HX-11	0.2	4.18E-07
HX-12	0.2	1.13E-07
HX-13	0.2	1.30E-07
HX-14	0.1	4.16E-07
HX-15	0.1	5.63E-07
HX-16	0.1	5.50E-07
HX-18	0.1	1.50E-06
HX-20	0.1	6.55E-06

where $h_{f,i}$ is the freshwater head of point i, h_i is the point water head of point i, ρ_i is the water density of point i, p_f is the freshwater density, and z_i is the level of the well screen at point i.

The vertical flow component of Darcy's Law should be converted into:

$$q_z = -K_f\left[\frac{\partial h_f}{\partial_z} + \left(\frac{\rho - \rho_f}{\rho_f}\right)\right] \tag{4}$$

where q_z is the vertical flux, K_f is the freshwater hydraulic conductivity, and the difference between K_f and the field-measured values of hydraulic conductivity is much smaller than the uncertainty associated with this parameter. Hence, no special corrections of existing hydraulic conductivity information are normally required.

The density of high-salinity groundwater can be calculated by:

$$\rho_w = 62.368 + 0.438603 \times 10^{-4} S + 1.6007410 \times 10^{-3}\left(10^{-4} S\right)^2 \tag{5}$$

where ρ_w is the density of groundwater (kg/m^3) and S is the total dissolved solids (TDS) content of groundwater (mg/l; Mccain 1991). The water densities of wells HX-14, HB2-15 and BJ2-1 are 1.04×10^3 kg/m^3, 1.10×10^3 kg/m^3 and 1.00×10^3 kg/m^3 respectively, which are used in later calculations and analysis.

Temperature tracing

Groundwater movement is accompanied by energy transfer. The combination of hydrogeological conditions and other external factors results in spatial and temporal variations in groundwater temperature that can support characterization of the groundwater movement. An understanding of the spatial and temporal distribution of temperature in the bottom of rivers, lakes, wetlands, and canals will facilitate definition of the exchange processes between groundwater and other water bodies. As a natural tracer, heat (represented by temperature) can be used to determine the direction and velocity of groundwater flow.

Because the HZ of Dakebo Lake is only several meters thick below the lake, and to account for the influence of the Earth's rotation and revolution, the surface temperature is assumed to comply with sinusoidal variation with time (Stallman 1965). The mathematical model of heat transport within the HZ was based on the one-dimensional (1D) steady-flow heat transport model established by Stallman (1965), as follows:

$$\frac{\lambda_e}{\rho c}\frac{\partial^2 T}{\partial z^2} - q\frac{\rho_w c_w}{\rho c}\frac{\partial T}{\partial z} = \frac{\partial T}{\partial t} \tag{6}$$

where T is the temperature (°C), t is the time (d), z is the thickness of the sediments (m), q is the water flow rate (m^3/day), ρ_w is the density of water (kg/m^3) and λ_e is the effective thermal conductivity of the saturated sediment (Stallman 1965).

The flow rates were calculated by the VFLUX program within MATLAB (Gordon et al. 2012). The following equation for temperature amplitude attenuation was used (Keery et al. 2007):

$$\left(\frac{H^3 D}{4z}\right)q^3 - \left(\frac{5H^2 D^2}{4z^2}\right)q^2 + \left(\frac{2HD^3}{z^3}\right)q + \left(\frac{\pi c\rho}{\lambda_e \tau}\right) - \frac{D^4}{z^4} = 0 \tag{7}$$

where $D = \ln\left(\frac{A_{z,t+\Delta t}}{A_{0,t}}\right)$, $H = \frac{c_w \rho_w}{\lambda_e}$, $A_{z,t+\Delta t}$, and $A_{0,t}$ are, respectively, the amplitudes of the oscillations of the single

frequency at a depth z and time $t + \Delta t$, and at a depth 0 and time t, where Δt is the time lag between oscillations at depths z and 0. The distance is z, q is positive in the z direction, ρ is the density of the saturated sediment, ρ_w is density of water, c is the specific heat capacity of the saturated sediment, c_w is the specific heat capacity of water, λ_e is the effective thermal conductivity of the saturated sediment, and τ is the time period.

For a given set of temperature time series from a single vertical sensor profile at a specific depth, the VFLUX program will (1) format and synchronize all the time series to a single vector of sampling times, (2) low-pass filter and resample the time series, (3) isolate the fundamental signal (the signal of interest, typically diurnal) using dynamic harmonic regression (DHR), (4) extract amplitude and phase information for the fundamental signal using DHR, (5) identify pairs of sensors based on one or more sliding analysis windows, and (6) calculate vertical water flux rates between the identified sensor pairs (Gordon et al. 2012).

Results and discussion

$\delta^{18}O$ and $\delta^{2}H$ of precipitation, lake water and groundwater

The hydrogen-oxygen stable isotope composition of precipitation varies between regions because of meteorological factors, latitude, altitude, precipitation, and evaporation conditions. Previous studies (Wang 2011) have shown that the hydrogen-oxygen stable isotope composition of precipitation in the Ordos Dakebo Lake region varies seasonally (Fig. 5). In this study, precipitation became more enriched with heavy hydrogen-oxygen stable isotopes from April to July, when the $\delta^{18}O$ value ranged from −6.8 to −5.4 ‰ and the $\delta^{2}H$ value ranged from −40 to −24 ‰. Conversely, they showed a relative loss from January to March and from August to October of each year, when the $\delta^{18}O$ value ranged from −10.2 to −7.1 ‰ and the $\delta^{2}H$ value ranged from −79 to −60 ‰.

The local meteoric water line, shown in Fig. 6, is plotted from the stable isotope data of 23 collected precipitation samples. As shown in Fig. 7, the $\delta^{18}O$ values of pore water in the HZ of HX increased from deep to shallow, indicating mixing between pore water and lake water. At HB1 and HB2, the $\delta^{18}O$ values of deep pore water were close to those of the surrounding groundwater, which indicates that the pore water came from the surrounding groundwater. As shown in Fig. 8, the $\delta^{18}O$ values peaked, and TDS reached 87 and 136 g/L, at depths of 0.7 and 1.2 m in HB1 and HB2, respectively, indicating that there were brine layers at these two depths. In HB1 and HB2 the water below the brine layer was a mixture of deep pore water and brine, while the water above the brine layer was a mixture of lake water, surrounding groundwater, and brine. At HX, the shallow groundwater was a mixture of lake water and deep groundwater.

As shown in Fig. 9, $\delta^{18}O$ and $\delta^{2}H$ values of the two lake-water samples (−4.45 ‰, −49.1 ‰ and −4.54 ‰, −49.4 ‰) were both distributed on the right side of the regional precipitation line, and were much higher than the values of precipitation in the region, reflecting the strong evaporation in the study area. The $\delta^{18}O$ and $\delta^{2}H$ values of the HZ pore water ranged from −5 to −10 ‰ and from −40 to 70 ‰, respectively, and were also distributed on the right side of the regional precipitation line. These values were evenly distributed on the line that connected the values of deep groundwater, lake water, and brine within the HZ, reflecting a mixing process between the different end-member waters. The values of the surrounding groundwater were on the regional precipitation line, which indicates that the surrounding groundwater was mainly recharged by precipitation.

Mixing ratio of groundwater and lake water within the HZ

The results of isotope studies support the idea that pore water in the HZ is formed by mixing of the different types of end-member water, and that differences in hydrodynamic and end member water at each location lead to different mixing patterns and ratios.

In particular, when calculating the mixing ratio of the end members HB1 and HB2, lake water and the surrounding groundwater were considered as one end member to mix with brine. The vertical distributions of the ratios of different end-member water bodies at different depths are shown in Fig. 10. The groundwater/lake-water interaction zone at HX ranges from the surface of the lakebed to about 1 m deep, with a lake water-mixing ratio of about 30 %.

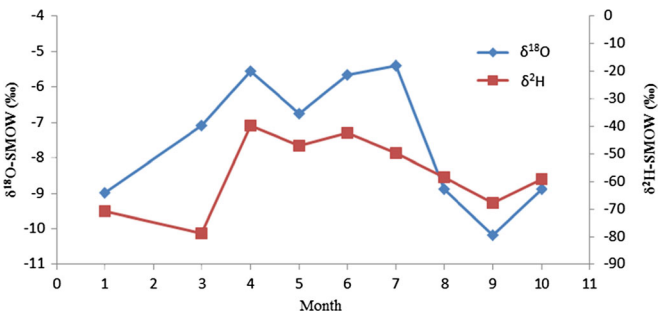

Fig. 5 Monthly variation in average $\delta^{18}O$ and $\delta^{2}H$ values of precipitation in the Dakebo Lake region

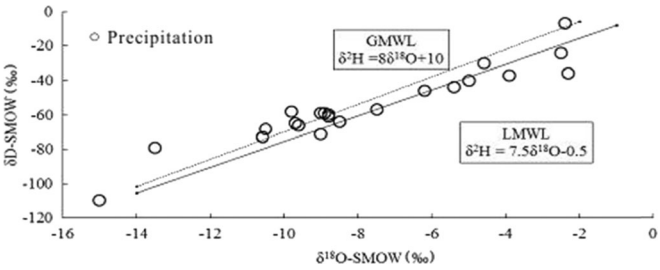

Fig. 6 Relationship between the $\delta^{18}O$ and $\delta^{2}H$ values of precipitation. (*GMWL*: global meteoric water line, *LMWL*: local meteoric water line)

The interactions were different at HB1 and HB2 because of lateral recharge from surrounding groundwater to pore water and mixing of residual brine and the overlying lake water. At HB1, the ratio of lake water and the surrounding groundwater at a depth of 0.7 m reached between 67 and 72 %, while the ratio of brine varied from 10 to 80 % at depths of between 0.7 and 2.5 m, and showed an increasing trend with proximity to the brine layer. At HB2, the ratio of lake water and surrounding groundwater increased from 20 to 98 % from 1.2 to 0 m deep to the surface of the lakebed, and the ratio of brine varied from 30 to 96 % between 1.2 and 3 m depth.

This analysis shows that the hydrodynamic intensity of pore water and the hydrodynamic exchange zones within the HZ at each location profile are determined by calculating the mixing ratio. The extent of the hydrodynamic exchange zone in the study area varied in the study area (Fig. 10). In this study, the hydrodynamic exchange zone ranged from the surface of the lakebed to 1.2 m below the lakebed surface at HX. This range increased on both sides of the lake, and extended from the lakebed surface to 2.5 m and to 4.5 m at HB1 and HB2, respectively. The difference in the ranges mainly reflects differences in hydrodynamic conditions. At the center of the lake, there is a lower hydraulic gradient, denser sediment media and weaker hydrodynamics than at either side of the lake, which leads to a smaller hydrodynamic exchange range.

Monitoring results of water level and temperature

Natural and human factors such as the annual ice period, strong evaporation, pumping, and brine evaporation, have strongly influenced the fluctuations in the lake-water and pore-water levels (Fig. 11). During winter, the pore water and lake water are frozen, which leads to large errors in the data from pressure-sensing automatic water-level recorders, resulting in disordered

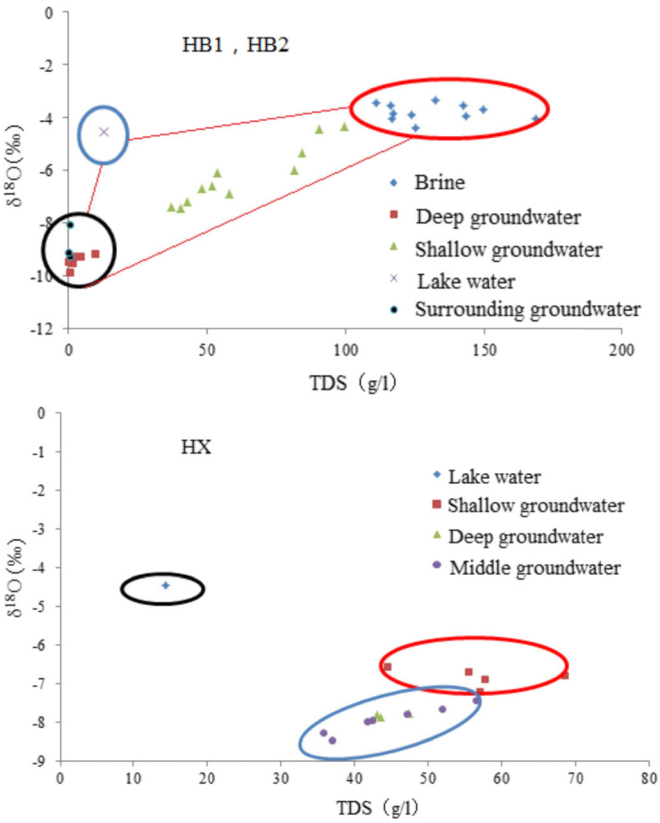

Fig. 7 Distribution of $\delta^{18}O$ and TDS in pore water within the lake HZ

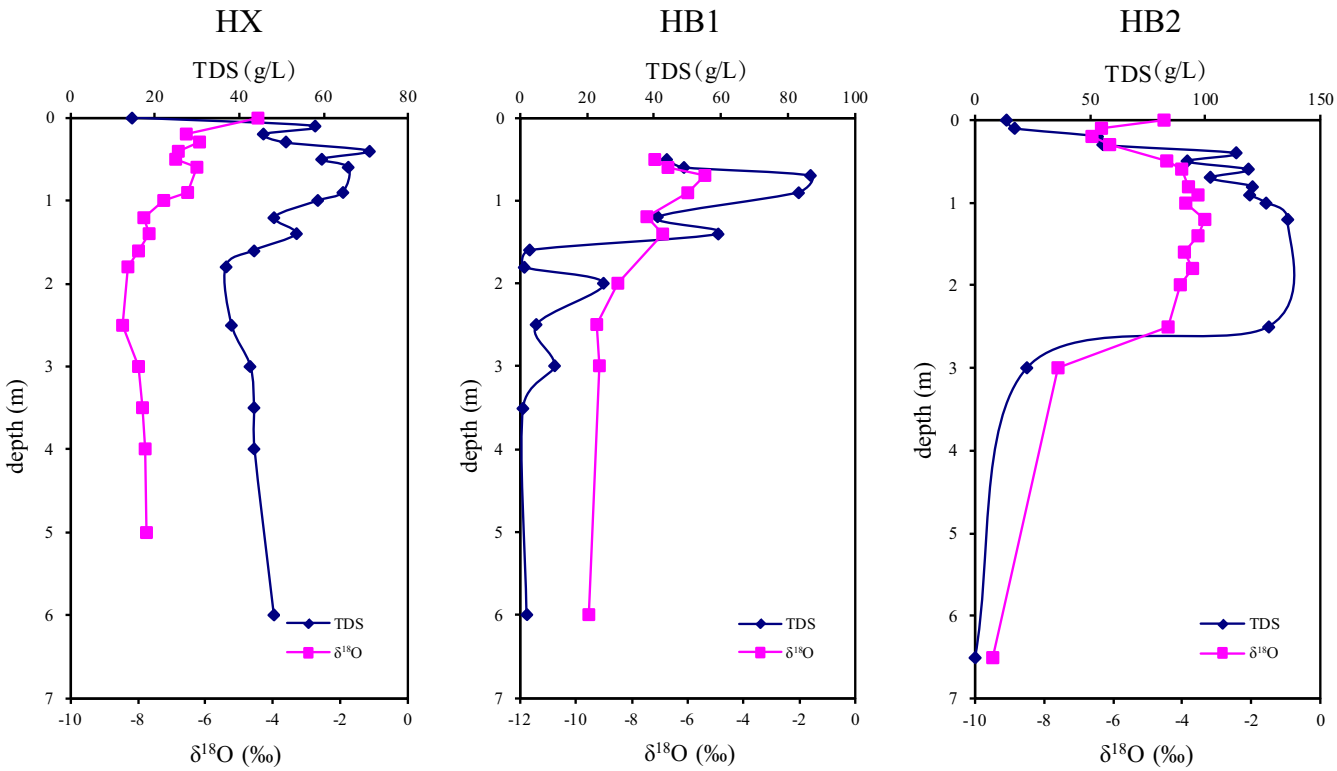

Fig. 8 Vertical distribution of $\delta^{18}O$ and TDS values of pore water within the HZ at the monitoring sites

data fluctuation. During the summer, water is frequently pumped from the lake into a pool by an alkali factory, so that the lake water heats up, with the result that alkali remains in the pool after the water evaporates. This process drains some parts of the lake and has an effect on the natural variation of the pore-water level within the HZ. Some lake-water-level data are missing because parts of the lake dry up during this process; therefore, the amount of exchange between groundwater and lake water during these two periods has been ignored.

At HB2, temperature fluctuations showed significant variation up to a depth of 1 m and the differences in amplitude between the sequences of adjacent depths were such that the amplitude method proposed by Hatch et al. (2006) could be used to calculate the flow rate within this range. Conversely, there was almost no fluctuation in temperature below 1 m and the amplitude was small, indicating that the exchange calculation method was not suitable for this range (Fig. 12).

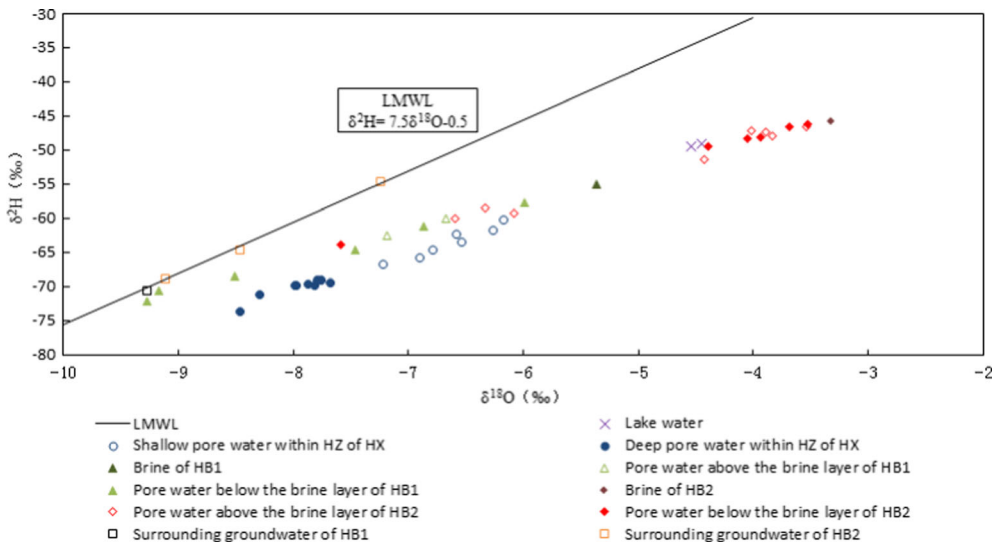

Fig. 9 Relationships between $\delta^{18}O$ and $\delta^{2}H$ in lake water, pore water, and surrounding groundwater at different monitoring sites within the saline lake

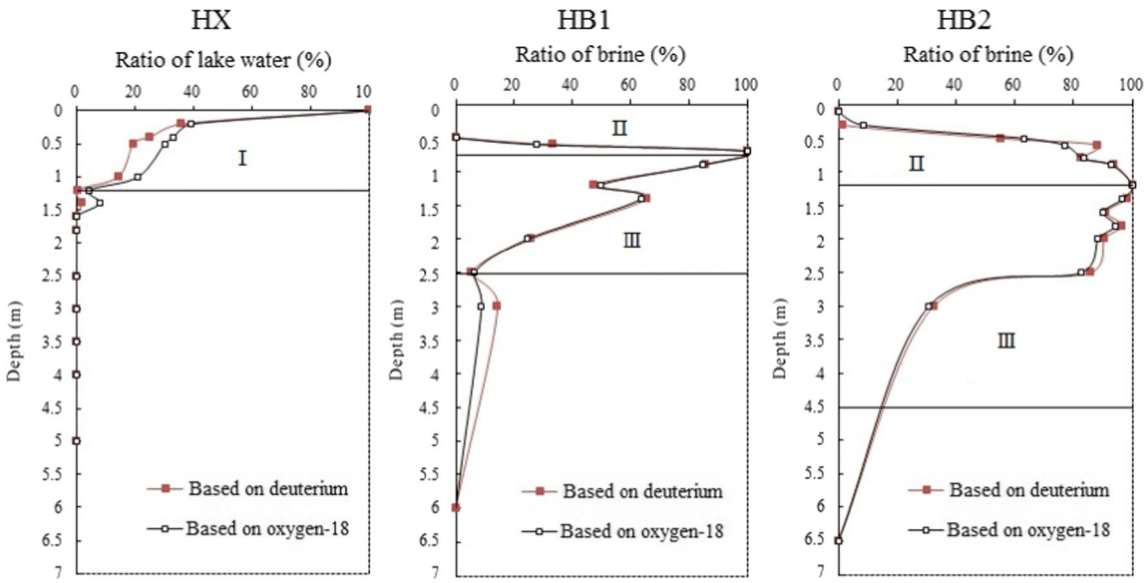

Fig. 10 Mixing ratios of different end-member water bodies in pore water at the monitoring sites of the Dakebo Lake region. (Range *I* is a mixture of pore water and lake water, range *II* is a mixture of surrounding groundwater, lake water, and brine, range *III* is a mixture of pore water and brine)

Groundwater/lake-water exchange flux

Based on the water level data, groundwater recharges the lake vertically at HX, with a hydrodynamic interaction zone ranging from the lakebed surface to a depth of about 1 m in the HZ. Therefore, the groundwater/lake-water exchange rate was calculated from the groundwater level data of HX-14 holes (1 m deep) and lake-water level data (Fig. 13).

The results show seasonal variation, and the flow rate ranged from 1.7×10^{-7} to 2.3×10^{-7} m/s during spring and autumn because of the low evaporation rates. Conversely, there were sharp declines in pore-water and lake-water levels during summer because of intense evaporation, water extraction, and brine evaporation processes, the flow rate then decreased to less than 0.5×10^{-7} m/s because there was almost no means of recharging the lake from the groundwater. During winter, the recharge was weak because of the ice period.

The hydrodynamic characteristics at HB2 differed from those at HX. At HB2, the lake is recharged by both vertical and lateral groundwater flow. The vertical flow rate was estimated using the groundwater level data from HB2-15 (0.9 m deep) and the lake-water level data, while the lateral flow rate was estimated using the groundwater level data of BJ2-1 (200 m from the lakeshore) and the lake-water level data (Figs. 14 and 15). The lateral groundwater flow rate at HB2 varied gradually during the year and ranged from 2×10^{-7} to 3×10^{-7} m/s.

Conversely, the vertical groundwater flow rate varied intensely during the year, and was around 3×10^{-6} m/s occurring around spring and autumn, but was only 2×10^{-6} m/s during summer because of the great decline in pore-water level and

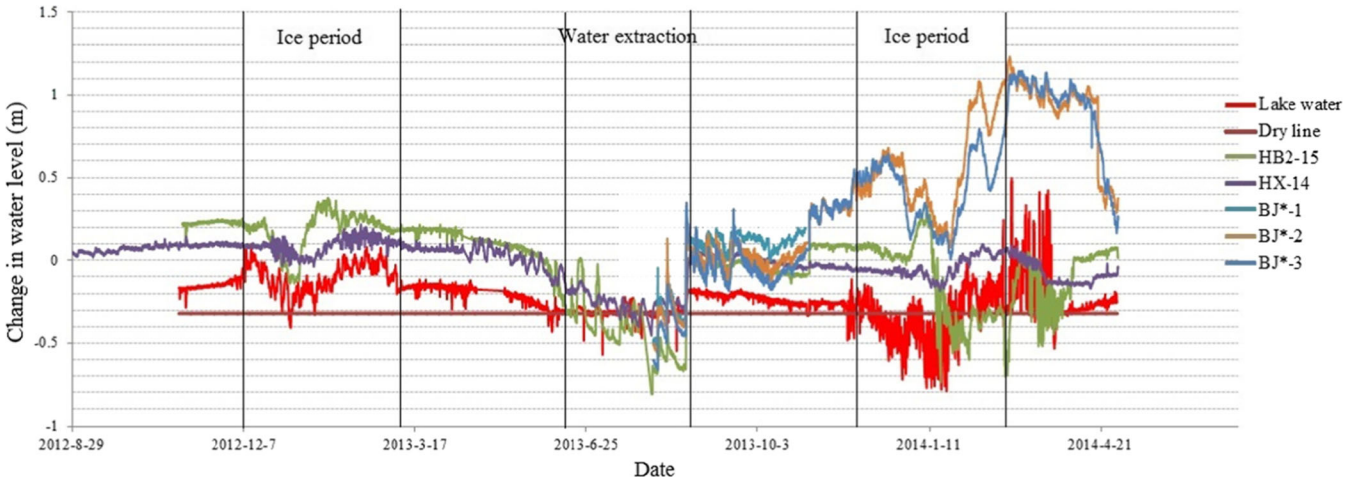

Fig. 11 Variations in lake-water level and pore-water level within the Dakebo Lake region (water heads of groundwater have been corrected to freshwater heads)

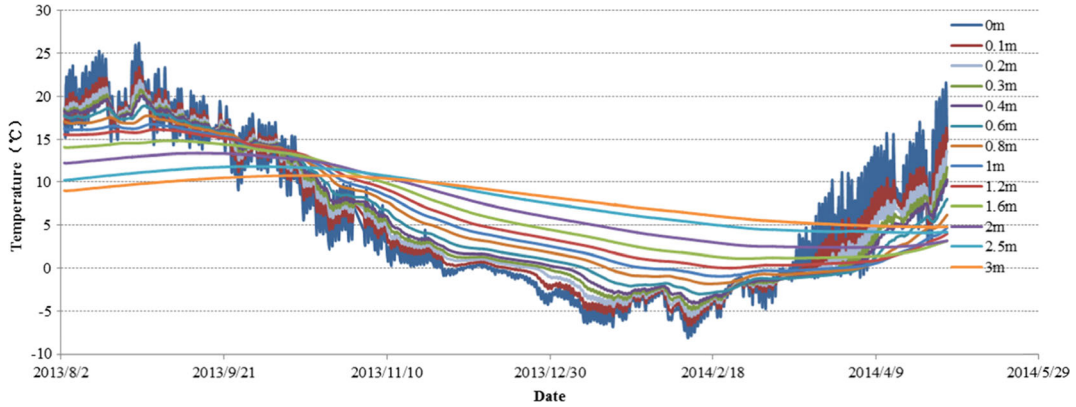

Fig. 12 Temperature fluctuations at different depths at HB2

lake-water level caused by natural and human factors, including strong evaporation and water extraction.

Groundwater discharge to Dakebo Lake varied throughout the year. During late spring and early summer, snowmelt recharged groundwater, which increased the surrounding water table and the hydraulic gradient. As a result, the recharge intensity increased under a hydraulic gradient of around 0.2–0.3. Conversely, the recharge intensity declined under a hydraulic gradient of around 0.01–0.1 in late summer, which was caused by water extraction and strong evaporation. In autumn, as evaporation weakened and precipitation recharged the groundwater during the rainy season of late summer (around August), the recharge intensity increased under a hydraulic gradient of 0.2–0.3. The recharge intensity became extremely weak in winter during the ice period when the water of the lake and the groundwater within a depth of 3 m were frozen.

There was considerable variation in the intensity of groundwater/lake-water exchange. The hydrodynamic conditions at the western side of the lake were stronger than in the center. The rate of the groundwater/lake-water exchange was about 10 times greater on the western side than at the center. This was caused by the finer sediments, lower hydraulic conductivity and lower hydraulic gradient at the center of the lake.

The results based on VFLUX are shown in Fig. 16. With proximity to the lakebed, the flow rate decreased because the mixing ratio of groundwater became smaller as groundwater moved closer to the lakebed. Additionally, differences in the flow rate at different depths reflected the heterogeneity of the sediment media. The flow rate calculated by the temperature tracing method therefore reflects the combination of various factors, including heterogeneity, anisotropy, groundwater density, specific heat of sediment media, and thermal conductivity. Examination of temporal variations showed that the groundwater flow rate varied from 0.5×10^{-6} to 3×10^{-6} m/s in summer and autumn. As shown in Fig. 16, there was almost no exchange between groundwater and lake water during winter. This was because the frozen soil in the study area extended to about 1.2 m, meaning that both the lake and the HZ were frozen. Therefore, the flow rate calculated for this period may not reflect the actual situation. In spring, the flow rate remained between 0.5×10^{-6} and 4×10^{-6} m/s.

The flow rate calculated by the hydrodynamic and temperature tracing methods approached each other and showed similar temporal variations, indicating that groundwater always recharges the lake water (Fig. 17).

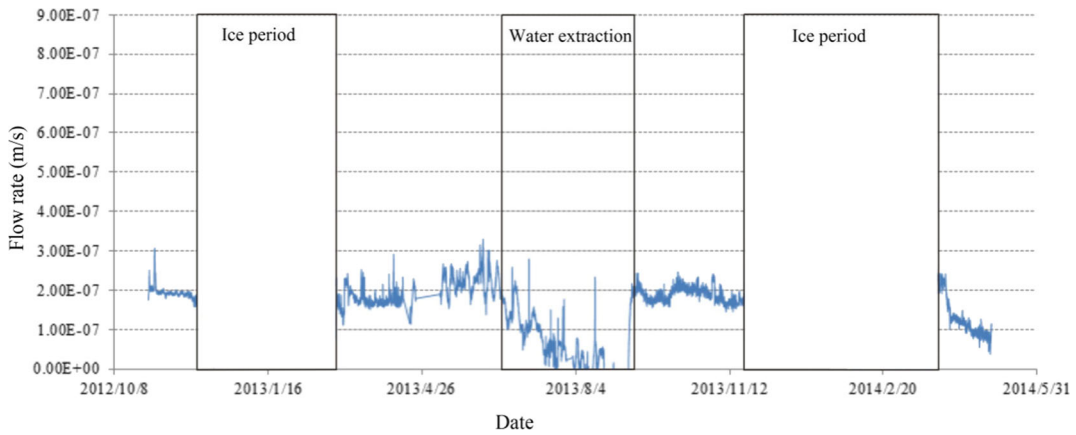

Fig. 13 Variation in vertical flow rate at point HX-14

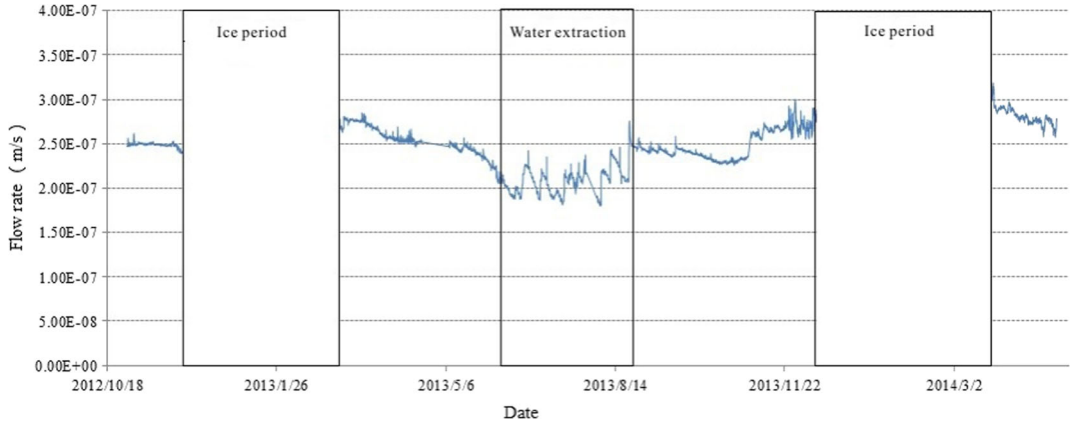

Fig. 14 Variation in lateral groundwater flow rate at point BJ2-1

As shown in the hydrogeological profile of the shallow Dakebo lakebed (Fig. 2), the sediment is mainly silty loam except for a 1-m thick layer of sand on part of the surface on the western side. Therefore, the lake should be divided into areas of different recharge rate so that the recharge quantity can be calculated more accurately. Dakebo Lake covers an area of 4 km^2, and the lakeshore covers 0.3 km^2, accounting for about 7 % of the total lake area. A rough average amount of groundwater discharge to the lake during 2012–2013, excluding the ice period from December to March, was estimated from the series data of groundwater flow rate in the west area of the lake at 1.0×10^7 m^3. The storage capacity of Dakebo Lake during 2012–2013 remained stable at about 0.1×10^7 m^3. These findings indicate that groundwater is an important source of recharge for Dakebo Lake. The water budget equation for Dakebo Lake is as follows:

$$Q_l + \Delta Q_l = Q_p + R - Q_e \quad (8)$$

where Q_l is the storage capacity of Dakebo Lake (0.1×10^7 m^3), ΔQ_l is the change in the lake water, Q_p is the amount of precipitation recharge (0.1×10^7 m^3), R is the amount of groundwater recharge (1.0×10^7 m^3), and Q_e is the amount of evaporation from the lake (1.0×10^7 m^3). The calculated ΔQ_l was 0 m^3, which indicates that the estimates of groundwater discharge to Dakebo Lake are reliable.

Conclusions

Hydrodynamic exchange characteristics within the HZ were determined from the hydrogen-oxygen stable isotopes in different water bodies. When the standard method for determining the HZ range is applied (Triska et al. 1993), water from the hydraulic exchange zone at the center of the lake (HX) at depths of 0–1.2 m below the lakebed is mainly a mixture of lake water and deep pore water. On the eastern and western sides (HB1, HB2) of the lake, the water of the hydraulic exchange zone , from the lakebed to depths of 2.5 and 4.5 m respectively, is a mixture of brine, lake water, and surrounding groundwater, below which there is a brine layer, then a mixture of deep pore water and brine. It is obvious that the difference in the range of the hydraulic exchange zone is caused by differences in the sediment structure and hydrodynamic conditions. The surface of the site HX is mainly composed of silty loam and a thin layer of clay loam with low permeability, while the surfaces at HB1 and HB2 mainly comprise sandy

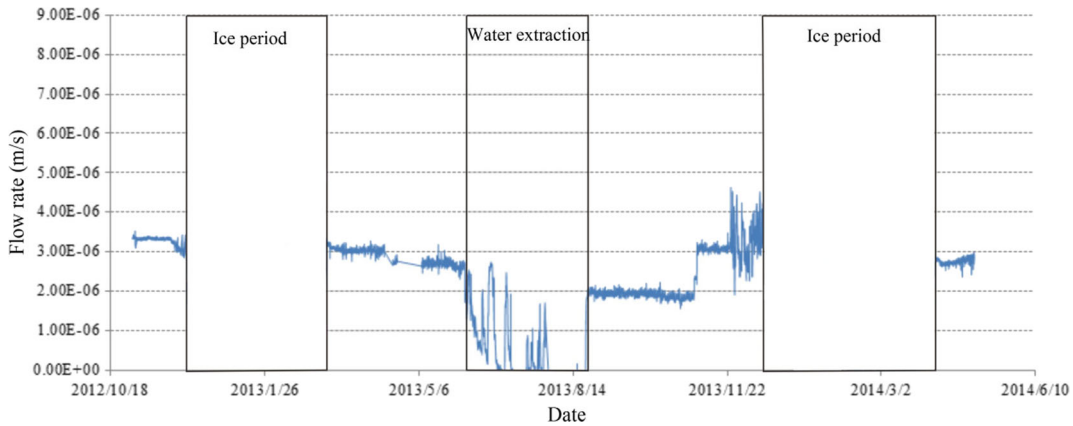

Fig. 15 Variation in vertical flow rate at point HB2-15

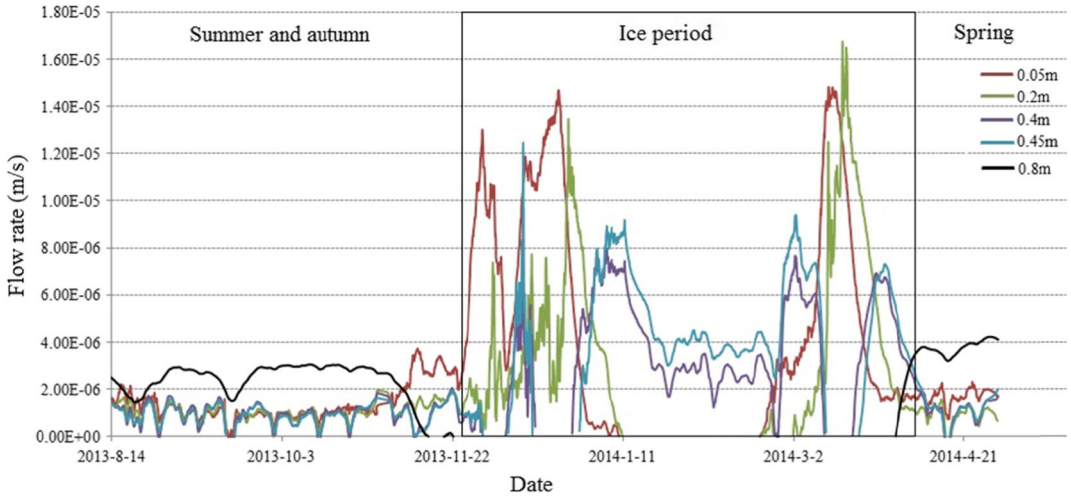

Fig. 16 Variation in vertical flow rate based on the temperature tracing method

loam and sand with reasonably high permeability. The exchange rate is higher at HB2 than at HX, which indicates that the hydrodynamic conditions are stronger at the lakeshore than in the center of the lake. These factors help to explain why the ranges in the hydraulic exchange zones are larger at HB1 and HB2 than at HX.

The groundwater/lake-water exchange rate was estimated from the hydrodynamic and temperature tracing methods. Results from the hydrodynamic method indicated that the vertical groundwater recharge rate at the center of the lake ranged from 1.7 to 2.3×10^{-7} m/s in spring and autumn, and was less than 0.5×10^{-7} m/s during summer. At the western side of the lake, the vertical rate increased to around 3×10^{-6} m/s in spring and autumn, and was 2×10^{-6} m/s in summer and the lateral groundwater recharge rate ranged from 2×10^{-7}–3×10^{-7} m/s. The recharge rate at the boundary of the lake was significantly greater, about 10 times greater than that at the center of the lake. The groundwater recharge rate estimated by the temperature tracing method varied from 0.5×10^{-6} to 4×10^{-6} m/s during spring, summer, and autumn. The traditional approach, based on Darcy's Law, was compared with three other non-traditional methods for measuring groundwater flow (stable isotope mass balance, temperature profile modeling, and numerical water balance modeling) in a groundwater-dominated natural and constructed wetland in southwestern Wisconsin, USA. Values obtained by methods other than Darcy's Law generally compared favorably and showed that there was groundwater flow from the deeper groundwater system at all three sites at rates of between 0.1 and 1.1 cm/day. Because of the error associated with some of the estimates, the groundwater inflow rates were thought to be slightly smaller, and ranged from 0.2 to 0.8 cm/day. The rate of groundwater inflow was generally greater at sites near the river regardless of the method (Hunt et al. 1996). As a form of wetland, the estimates of groundwater recharge rate for Dakebo Lake calculated in this

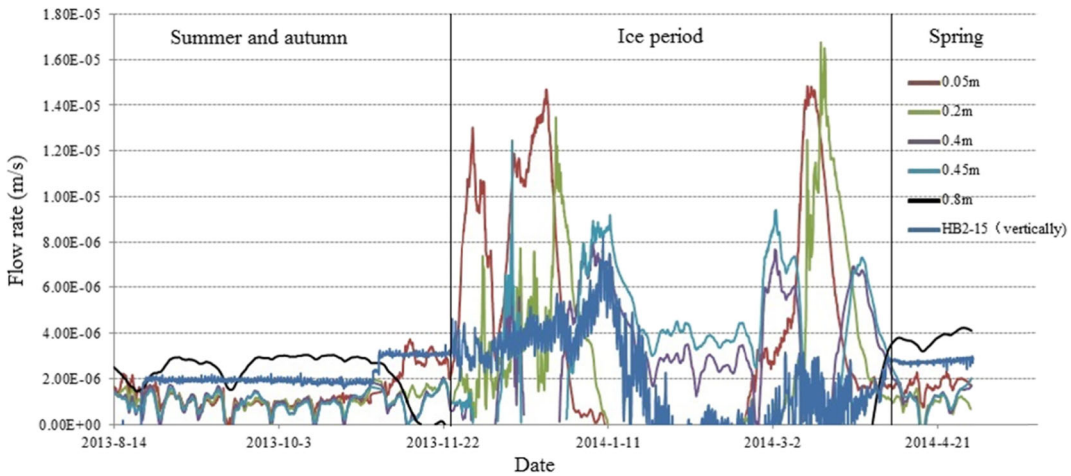

Fig. 17 Comparison between the hydrodynamic and temperature tracing methods (*HB2-15* represents the results of the hydrodynamic method and the *other lines* represent the results of the temperature tracing method at different depths)

study are similar to the results calculated by Hunt et al. (1996) using similar approaches.

The average amount of groundwater recharge in the lake during 2012–2013, excluding the ice period from December to March, was estimated at approximately 1.0×10^7 m^3. Conversely, the storage capacity of Dakebo Lake remained stable at around 0.1×10^7 m^3 from 2012 to 2013. The groundwater recharge quantity was 10 times greater than that of the lake storage capacity, indicating that groundwater is an important source of water recharge in Dakebo Lake.

Acknowledgements This work was funded by the National Natural Science Fund Project "Research in biogeochemical behavior of sulfur within desert plateau hypolentic zone" (Grant No. 41073054). The authors would like to thank the editor, associate editor, Perry de Louw and the anonymous reviewers for their thoughtful and constructive comments, which helped improve the manuscript.

References

Cao Y (2009) Groundwater circulation patterns of typical lake area in northern Ordos cretaceous basin (in Chinese). MSc Thesis, Jilin University, China

Carey SK, Quinton WL (2005) Evaluating runoff generation during summer using hydrometric, stable isotope and hydrochemical methods in a discontinuous permafrost alpine catchment. Hydrol Process 19(1):95–114

Constantz JE, Niswonger RG, Stewart AE (2008) Analysis of temperature gradients to determine stream exchanges with ground water. Econ Hist Rev 23(1):96–111

Du SH, Su XS, Zhang WJ (2013) Effective storage rates analysis of groundwater reservoir with surplus local and transferred water used in Shijiazhuang City, China. Water Environ J 27: 157–169

Elsawwaf M, Feyen J, Batelaan O, Bakr M (2014) Groundwater–surface water interaction in Lake Nasser, South Egypt. Hydrol Process 28: 414–430

Essaid HI, Zamora CM, McCarthy KA, Vogel JR, Wilson JT (2008) Using heat to characterize streambed water flux variability in four stream reaches. J Environ Qual 37(3):1010–1023

Fan W, Zhang GX, Li RR (2012) Review of groundwater–surface water interactions in wetlands. Adv Earth Sci 27:413–423

Gandy CJ, Smith JWN, Jarvis AP (2007) Attenuation of mining-derived pollutants in the hyporheic zone: a review. Sci Total Environ 373: 435–446

Gordon RP, Lautz LK, Briggs MA, Mckenzie JM (2012) Automated calculation of vertical pore-water flux from field temperature time series using the VFLUX method and computer program. J Hydrol 420(4):142–158

Grimm NB, Fisher SG (1984) Exchange between interstitial and surface water: implications for stream metabolism and nutrient cycling. Hydrobiologia 111(3):219–228

Guo J (2012) Research on sulfur biogeochemistry in hypolentic zone of lake in Kubuqi Desert plateau area. Jilin University, Changchun, China

Hatch CE, Fisher AT, Revenaugh JS, Constantz J, Ruehl C (2006) Quantifying surface water–groundwater interactions using time series analysis of streambed thermal records: method development. Water Resour Res 42(10):2405–2411

Hunt RJ, Krabbenhoft DP, Anderson MP (1996) Groundwater inflow measurements in wetland systems. Water Resour Res 32(3):495–507

Kalbus E, Reinstorf F, Schirmer M (2006) Measuring methods for groundwater–surface water interactions: a review. Hydrol Earth Syst Sci Discuss 10(6):873–887

Keery J, Binley A, Crook N, Smith JWN (2007) Temporal and spatial variability of groundwater–surface water fluxes: development and application of an analytical method using temperature time series. J Hydrol 336(1–2):1–16

Lee J, Robinson C, Couture RM (2014) Effect of groundwater–lake interactions on arsenic enrichment in freshwater beach aquifer. Environ Sci Technol 48:10174–10181

Li PY, Wu JH, Qian H (2016) Preliminary assessment of hydraulic connectivity between river water and shallow groundwater and estimation of their transfer rate during dry season in the Shidi River, China. Environ Earth Sci 75(2):99

Marimuthu S, Reynolds DA, La Salle CLG (2005) A field study of hydraulic, geochemical and stable isotope relationships in a coastal wetlands system. J Hydrol 315(1):93–116

Mccain WD (1991) Reservoir-fluid property correlations: state of the art (includes associated papers 23583 and 23594). SPE Reserv Eng 6: 266–272

Oyarzún R, Barrera F, Salazar P, Maturana H, Oyarzún J (2014) Multimethod assessment of connectivity between surface water and shallow groundwater: the case of Limarí River basin, north-central Chile. Hydrogeol J 22(8):1857–1873

Post V, Kooi H, Simmons C (2007) Using hydraulic head measurements in variable-density ground water flow analyses. Ground Water 45(6):664–671

Rau GC, Andersen MS, McCallum AM, Roshan H, Acworth RI (2014) Heat as a tracer to quantify water flow in near-surface sediments. Earth Sci Rev 129:40–58

Rautio A, Korkka-Niemi K (2015) Chemical and isotopic tracers indicating groundwater/surface-water interaction within a boreal lake catchment in Finland. Hydrogeol J 23:687–705

Rodríguez-Rodríguez M, Benavente J, Julián CS, Martos FM (2006) Estimation of ground-water exchange with semi-arid playa lakes (Antequera region, southern Spain). J Arid Environ 66(2):272–289

Sedell JR, Reeves GH, Hauer FR, Stanford JA, Hawkins CP (1990) Role of refugia in recovery from disturbances: modern fragmented and disconnected river systems. Environ Manag 14(5):711–724

Shaw GD, White ES, Gammons CH (2013) Characterizing groundwater–lake interactions and its impact on lake water quality. J Hydrol 492: 69–78

Sophocleous M (2002) Interactions between groundwater and surface water: the state of the science. Hydrogeol J 10(1):52–67

Stallman RW (1965) Steady one-dimensional fluid flow in a semi-infinite porous medium with sinusoidal surface temperature. J Geophys Res 70:2821–2827

Storey RG, Howard KWF, Dudley WD (2003) Factors controlling riffle-scale hyporheic exchange flows and their seasonal changes in a gaining stream: a three-dimensional groundwater flow model. Water Resour Res 39(39):180–189

Su XS, Wang XY, Wan YY, Cao Y (2011) Research on interaction of surface water and groundwater of Dakebo Lake watershed. Yellow River 33(7):73–75

Su XS, Xu W, Du SH (2014a) In situ infiltration test using a reclaimed abandoned river bed: managed aquifer recharge in Shijiazhuang City, China. Environ Earth Sci 71(12):5017–5025

Su XS, Xu W, Du SH (2014b) Responses of groundwater vulnerability to artificial recharge under extreme weather conditions in Shijiazhuang City, China. J Water Supply Res Technol 63(3):224–238

Su XS, Yuan WZ, Xu W, Du SH (2015) A groundwater vulnerability assessment method for organic pollution: a validation case in the Hun River basin, northeastern China. Environ Earth Sci 73(1):467–480

Triska FJ, Duff JH, Avanzino RJ (1993) Patterns of hydrological exchange and nutrient transformation in the hyporheic zone of a gravel-bottom stream: examining terrestrial—aquatic linkages. Freshw Biol 29(2):259–274

Wang X (2011) Research on groundwater circulation and hydrochemical evolution in Dakebo lake Watershed in Ordos Basin. Jilin University, Changchun, China

Wang X, Ouyang Z, Miao H (2003) Formation, evolution and protection of wetland ecosystems in arid region, northwestern China. Territory Nat Res Study 4:52–54

Yin L, Hou G, Su XS, Wang D, Dong J, Hao Y, Wang X (2011) Isotopes (δD and $\delta^{18}O$) in precipitation, groundwater and surface water in the Ordos Plateau, China: implications with respect to groundwater recharge and circulation. Hydrogeol J 19(2): 429–443

Zalewski M (2000) Ecohydrology: the scientific background to use ecosystem properties as management tools toward sustainability of water resources. Ecol Eng 16(1):1–8